

Formation of hard VHE gamma-ray spectra of blazars due to internal photon-photon absorption

Felix A. Aharonian^{*1,2}, D.Khangulyan² & L. Costamante³

¹*Dublin Institute for Advanced Studies, 31 Fitzwilliam Place, Dublin 2, Ireland*

²*Max Planck Institut für Kernphysik, Saupfercheckweg 1, D69117 Heidelberg, Germany*

³*Stanford University, W.W. Hansen Experimental Physics Laboratory & Kavli Institute for Particle Astrophysics and Cosmology, Stanford, CA 94305-4085, USA*

Accepted. Received; in original form

ABSTRACT

The energy spectra of TeV gamma-rays from blazars, after being corrected for intergalactic absorption in the Extragalactic Background Light (EBL), appear unusually hard, a fact that poses challenges to the conventional models of particle acceleration in TeV blazars and/or to the EBL models. In this paper we show that the internal absorption of gamma-rays caused by interactions with dense narrow-band radiation fields in the vicinity of compact gamma-ray production regions can lead to the formation of gamma-ray spectra of an almost arbitrary hardness. This allows significant relaxation of the current tight constraints on particle acceleration and radiation models, although at the expense of enhanced requirements to the available nonthermal energy budget. The latter, however, is not a critical issue, as long as it can be largely compensated by the Doppler boosting, assuming very large (≥ 30) Doppler factors of the relativistically moving gamma-ray production regions. The suggested scenario of formation of hard gamma-ray spectra predicts detectable synchrotron radiation of secondary electron-positron pairs which might require a revision of the current “standard paradigm” of spectral energy distributions of gamma-ray blazars. If the primary gamma-rays are of hadronic origin related to pp or $p\gamma$ interactions, the “internal gamma-ray absorption” model predicts neutrino fluxes close to the detection threshold of the next generation high energy neutrino detectors.

keywords: BL Lacertae objects: general, gamma-rays: theory, gamma-rays: observations, diffuse radiation

1 INTRODUCTION

The recent reports on detections of very high energy (VHE) gamma-rays from blazars with redshifts $z \geq 0.1$ (for a review see e.g. Hinton (2007)) initiated renewed debates on the interpretation of TeV gamma-ray spectra of blazars, in particular in the context of the level of the diffuse extragalactic background radiation at optical and infrared wavelengths, often called also as Extragalactic Background Light (EBL). Initially, the tight link between these two topics - TeV blazars and EBL - became a subject of hot discussions prompted by multi (up to 20) TeV gamma-rays detected from a nearby BL Lac object, Mkn 501 (Aharonian et al. 1999), and by the reports claiming detection of high fluxes of EBL at far infrared wavelengths (Hauser et al. 1998; Schlegel et al. 1998; Lagage et al. 1999; Finkbeiner et al. 2000). However, it was quickly recognised that these two claims hardly could be compatible within any standard model of TeV blazars (see, for a review, Aharonian (2001)).

A distinct feature of extragalactic gamma-ray as-

tronomy is that VHE gamma-rays emitted by distant (≥ 100 Mpc) objects arrive after significant absorption caused by their interactions with EBL via the process $\gamma\gamma \rightarrow e^+e^-$ (Nikishov 1962; Jelley 1966; Gould and Schröder 1967). The reconstructed, i.e. the absorption-corrected gamma-ray spectrum from a source at a redshift z , $J_0(E) = J_{\text{obs}}(E)e^{\tau(E,z)}$ depends on the flux and energy spectrum of EBL through the optical depth $\tau(E, z)$. Thus, at energies where $\tau(E, z) \geq 1$, the primary gamma-rays suffer strong spectral deformation.

The EBL consists of two emission components produced by stars and partly absorbed/re-emitted by dust throughout the entire history of galaxy evolution. As a result, two distinct bumps are expected in the spectral energy distribution (SED) of EBL at near infrared (NIR) and far infrared (FIR) wavelengths, with a mid-infrared (MIR) “valley” between these two bumps (see e.g. Hauser and Dwek (2001)). Generally, for almost all EBL models, $\tau(E)$ is a strong function of energy below 1 TeV and above 10 TeV; between 1 and 10 TeV the energy-dependence of $\tau(E)$ is much weaker (Aharonian 2001). Consequently, one should expect significant distortion of the VHE spectra of blazars at energies below 1 TeV and above 10 TeV, provided that at these energies $\tau \geq 1$. One can re-formulate this statement in a different way. Namely, for a standard (“decent”) intrinsic

gamma-ray spectrum, the observer should detect very soft (steep) spectra at energies below 1 TeV and above 10 TeV from objects for which $\tau \geq 1$ at corresponding energies. This condition is safely satisfied, given the constraints on the minimum EBL flux imposed by galaxy counts, for blazars with redshifts $z \geq 0.15$ like 1ES 1101-232 and for nearby objects with $z \sim 0.03$ like Mkn 501. Even though the *detected* gamma-ray spectra from both objects in the corresponding energy intervals are indeed quite steep with a photon index ~ 3 (Aharonian et al. 1999; Aharonian et al. 2006a), they appear not sufficiently steep to compensate the function $f(E) = e^{\tau(E)}$, and thus to prevent a robust conclusion that the *intrinsic* VHE gamma-ray spectra of these blazars are unusually hard.

In the case of Mkn 501, the intrinsic spectrum has a “non-standard” shape with a possible pile-up above 10 TeV which has been interpreted as a “IR background - TeV gamma-ray crisis” (Protheroe and Meyer 2000) or a need to invoke dramatic assumptions like a violation of the Lorentz invariance (see e.g. Kifune (1999)). However, a more pragmatic view which presently dominates in both infrared and gamma-ray astronomical communities, treats this “crisis” as somewhat exaggerated, especially given the ambiguity of extraction of the truly diffuse extragalactic FIR component from the much higher backgrounds of local origin (see e.g. Hauser and Dwek (2001)). Nevertheless, the recently reported low limits on the EBL at mid infrared wavelengths from the Spitzer deep cosmological surveys appeared quite high, for example at $70 \mu\text{m}$ the EBL flux should exceed $\geq 7.1 \pm 1.0 \text{ nW/m}^2\text{s}$ (Dole et al. 2006). This implies that the problem is not yet over, and one may still face a challenge with the interpretation of the energy spectra of Mkn 501 and Mkn 421 in the multi-TeV energy domain.

On the other hand, the recent detections of TeV gamma-rays from blazars with redshifts $z \geq 0.15$ renewed the potential problems and challenges for standard models of TeV blazars. This time the issue has a more solid experimental background, because the gamma-ray spectra corrected for the intergalactic absorption appear very hard (“harder than should be”) even for the minimum possible EBL fluxes at optical and NIR wavelengths. Namely, the HESS collaboration reported, based on the detection of TeV gamma-rays from the BL Lac object 1ES 1101-232, that any significant deviation from the lower limits of EBL determined by the integrated light of galaxies resolved by the Hubble telescope (Madau and Pozzetti 2000), would lead to very hard intrinsic gamma-ray spectrum with a slope characterized by a photon index $\Gamma_0 \leq 1.5$ (Aharonian et al. 2006a). The analysis based on a larger sample of TeV blazars leads to the same conclusion (Mazin and Raue 2007). Recently, the HESS collaboration reported detection of multi-TeV gamma-rays from 1ES 0229+200, a BL Lac object located at a redshift $z=0.1396$ (Aharonian et al. 2007a). It is remarkable that the *detected* hard gamma-ray spectrum of this source with a photon index $\Gamma_{\text{obs}} \sim 2.5$ extends up to 15 TeV. This, to a certain extent surprising result can be explained by the shape of the energy flux of EBL which between the NIR and MIR bands is expected to be proportional to λ^{-1} (Aharonian 2001). Yet, the absolute EBL flux, derived from a rather conservative assumption that the photon index of the intrinsic spectrum of TeV gamma-rays does not exceed 1.5, appears again close to the EBL lower limit, this time

at MIR ($\approx 2 - 3 \text{ nW/m}^2\text{sr}$ at $10 \mu\text{m}$), derived from the Spitzer galaxy counts (Fazio et al. 2004; Dole et al. 2006). Thus, the gamma-ray observations of 1ES 1101-232 and 1ES 0229+200 can be interpreted as an argument that the galaxies resolved by the Hubble and Spitzer telescopes provide the bulk of the EBL flux from optical to mid infrared wavelengths. Given the importance of such a statement, in particular for understanding of contribution of the first stars to the EBL (see e.g. Kashlinsky (2005); Mapelli et al. (2006)), it is essential to explore alternative ways of explanation of very hard intrinsic gamma-ray spectra or even sharper spectral features (like pile-ups) in TeV blazars. In this context, recently some extreme assumptions regarding the distributions of accelerated particles have been proposed. In particular, Katarzynski et al (2006) argued that a gamma-ray spectrum as hard as $\Gamma_0 \sim 0.7$ can be formed in a SSC model assuming a narrow parent electron distribution, e.g. power-law within E_1 and E_2 , with a low-energy cutoff E_1 not much smaller than the high energy cutoff, E_2 . In similar lines, Stecker et al (2007) argued that electron spectra with power law index ≤ 1 can be accommodated within the models of relativistic shock acceleration. It should be noted, however, that in compact objects relativistic electrons usually suffer very fast synchrotron losses, therefore the assumptions about hard electron *acceleration* cannot yet guarantee hard gamma-ray spectra. Indeed, the radiatively cooled electron spectrum cannot be harder than $dN/dE \propto E^{-2}$, independent of the initial (acceleration) spectrum (see e.g. Aharonian 2004). If so, the inverse Compton scattering would result in a gamma-ray spectrum steeper than $E^{-1.5}$. In fact, the Klein-Nishina effect makes the spectrum even steeper. In principle, one can avoid the synchrotron cooling of electrons, e.g. in a cold ultrarelativistic wind. However such a hypothesis suggested for Mkn 501 (Aharonian et al. 2002), in analogy with pulsar winds, needs thorough theoretical studies to clarify whether such cold ultrarelativistic winds can be formed and survived around supermassive black holes in the cores of AGN.

In this paper we suggest a new scenario which allows formation of very (in practice, arbitrary) hard gamma-ray spectra in a quite natural way. The model is based on a postulation that gamma-rays before leaving the source suffer significant photon-photon absorption due to interactions with dense radiation fields inside or in the vicinity of compact gamma-ray production region(s). Interestingly, the presence of high density radiation fields of different origin in the inner parts of blazars generally is treated as a problem for the escape of high energy gamma-radiation from their production region, and, in this regard, the current models of TeV blazars are designed in a way to avoid the internal gamma-ray absorption. Below we show that, in fact, a moderate internal photon-photon absorption can be a clue to the very hard intrinsic energy spectra of TeV blazars.

2 INTERNAL ABSORPTION OF GAMMA-RAYS IN BLAZARS

When propagating through an isotropic source of low-frequency radiation, the gamma-ray absorption at photon-photon interactions is characterized by the optical depth

$$\tau(E) = \int_0^R \int_{\epsilon_1}^{\epsilon_2} \sigma(E, \epsilon) n_{\text{ph}}(\epsilon, r) d\epsilon dr, \quad (1)$$

where $n_{\text{ph}}(\epsilon, r)$ describes the spectral and spatial distributions of target photons in the source of size R . With a good accuracy, the total cross-section in the monoenergetic isotropic photon field can be represented in the form (see e.g. Aharonian 2004):

$$\sigma_{\gamma\gamma} = \frac{3\sigma_T}{2s^2} \left[\left(s + \frac{1}{2} \ln s - \frac{1}{6} + \frac{1}{2s} \right) \ln(\sqrt{s} + \sqrt{s-1}) - \left(s + \frac{4}{9} - \frac{1}{9s} \right) \sqrt{1 - \frac{1}{s}} \right]. \quad (2)$$

The cross section depends only on the product of the primary (E) and target photon (ϵ) energies, $s = E\epsilon/m_e^2 c^4$. Close to the threshold, $s \rightarrow 1$, the pair production cross-section behaves as $\sigma_{\gamma\gamma} \approx (1/2)\sigma_T(s-1)^{3/2}$. The cross-section decreases with s also when $s \gg 1$: $\sigma_{\gamma\gamma} \approx (2/3)\sigma_T s^{-1} \ln s$. The cross-section achieves its maximum at $s \approx 3.5$: $\sigma_{\gamma\gamma} \approx 0.2\sigma_T$.

For a homogeneous source with a narrow spectral distribution of photons, for order of magnitude estimates one can use the approximation $\tau(E) \simeq R\sigma_{\gamma\gamma}(E, \bar{\epsilon})n(\bar{\epsilon})$. In this case we should expect maximum absorption effect at gamma-ray energy $E^* \approx m_e^2 c^4 / \bar{\epsilon}$. Both at lower and higher energies, the source becomes more transparent, thus we should expect a quite strong deformation of the primary spectrum. In the case $\tau(E^*) \geq 1$, the effect could be dramatic, given the exponential dependence of the absorption on the optical depth. Note that while for a narrow spectral distribution of target photons the monoenergetic approximation gives a quite accurate estimate of the effect at $E \gg E^*$, at low energies, $E \leq 1/4E^*$, this approximation implies a completely transparent source (i.e. $\tau = 0$) although, a non-negligible absorption can take place also below E^* . For example, because of interactions with the Wien tail, the absorption effect in the black-body radiation field cannot be disregarded even at very low energies, $E \ll m_e^2 c^4 / kT$.

In Fig.1 (upper panel) we present the gamma-ray attenuation factor, $\kappa = \exp(-\tau)$ in a grey-body radiation field described by Planckian distribution with three different temperatures $T = 10^3$ K, 10^4 K, and 10^5 K calculated for an optical depth fixed at the energy corresponding to the maximum absorption, $E^* \approx m_e^2 c^4 / kT$ (Gould and Schröder 1967): Since the optical depth is a function of the product $E \cdot kT$, three curves are identical, but shifted relative to each other by a factor proportional to the radiation temperature. In Fig.1 we show also the attenuation factors for a fixed temperature $T = 10^4$ K calculated for three different optical depths $\tau_{\text{max}} = 0.5, 3$, and 6 . It is seen that the gamma-ray attenuation, starting from the energy $E \sim 0.1E^*$, gradually increases up to $E \sim E^*$, after which the source becomes more and more transparent ($\kappa \propto \exp[-E^{-1} \ln E] \rightarrow 1$), and, consequently, the primary spectrum starts to recover. As a result, in this energy interval the spectrum appears harder than the primary spectrum. The bottom panel of Fig.1 shows the change of the slope of gamma-ray spectrum, $\Delta\Gamma$, which can be interpreted as a change of the local photon index, assuming that the initial gamma-ray spectrum is described by a power-law distribution, $dN/dE \propto E^{-\Gamma_0}$. The emerging spectrum of gamma-

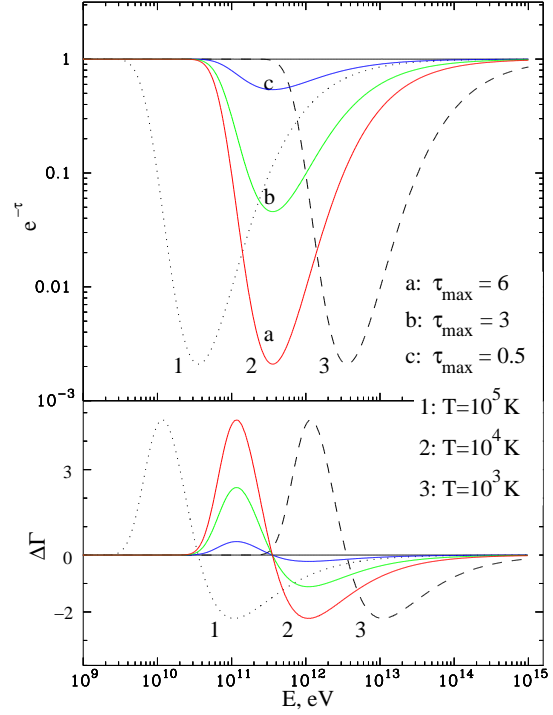


Figure 1. *Upper panel:* Attenuation factor $\kappa = \exp(-\tau)$ for three different temperatures of target photons, $T = 10^3$ K, 10^4 K, and 10^5 K (for the optical depth $\tau_{\text{max}} = 6$). For $T = 10^4$ K calculations are performed for three different optical depths: $\tau_{\text{max}} = 0.5$ (blue), 3 (green), 6 (red). *Bottom panel:* Variation of the local photon index of the gamma-ray spectrum.

rays in the energy interval $(0.1 - 1)E^*$ is steeper than the initial spectrum ($\Delta\Gamma \geq 0$); it recovers at $E = E^*$ ($\Delta\Gamma = 0$), and at energies $E \geq E^*$ the spectrum becomes significantly harder than the initial spectrum ($\Delta\Gamma \leq 0$). For example, in the case of initial gamma-ray spectrum E^{-2} and $\tau_{\text{max}} = 6$, the emerging spectrum of gamma-rays in the energy interval $(1 - 10)E^*$ can be very hard with $\Gamma = \Gamma_0 + \Delta\Gamma \sim 0$, although the absolute flux is suppressed by an almost three orders of magnitude at $E = E^*$, and an order of magnitude at $E = 10E^*$.

Note that the requirement of a narrow spectral distribution of the target photons is a key condition for this remarkable effect. It should not necessarily be a Planckian or monoenergetic distribution, but may have any other shape, for example power-law with a low-energy cutoff: $n(\epsilon) \propto \epsilon^{-\alpha}$ at $\epsilon \geq \epsilon_1$, and $n(\epsilon) = 0$ at $\epsilon \leq \epsilon_1$. In this case, the low-energy cutoff ϵ_1 plays a similar role as the temperature in the Planckian distribution. This is demonstrated in Fig. 2 for a power-law distribution of the background field with $\alpha = 2$ and sharp cutoff at $\epsilon_1 = 1$ eV and 10^{-3} eV. Indeed, for the same $\tau_{\text{max}} = 6$, the case of $\epsilon_1 = 1$ eV is quite similar to the case of Planckian distribution with temperature $T = 10^4$ K shown in Fig.1. The main difference appears in the low-energy part, $E \ll E^*$. The absorption curve in Fig.2 at low energies is smoother, because the $n(\epsilon) \propto \epsilon^{-2}$ type distribution provides more high-energy target photons compared to the Wien tail of the thermal distribution, for interactions with low-energy gamma-rays.

The hardening of the initial spectrum caused by internal absorption compensates, to a large extent, the steepen-

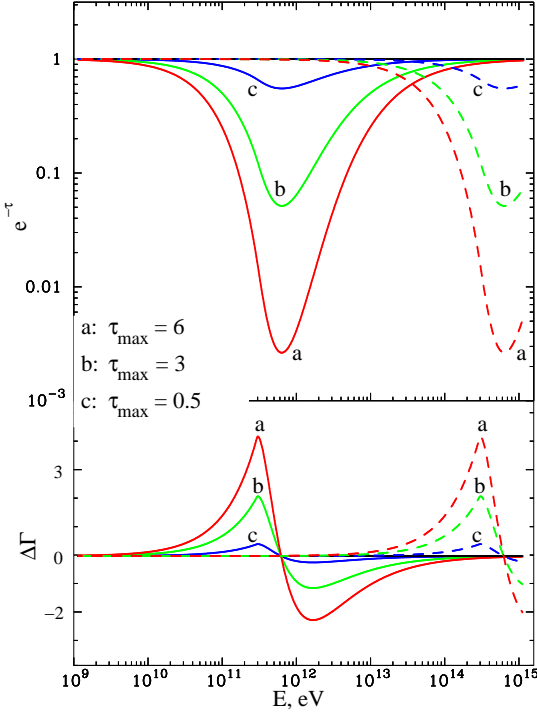


Figure 2. *Upper panel:* Attenuation factor calculated for a power-law distribution of target photons with a low-energy cutoff: $n_{\text{ph}} \propto \varepsilon^{-2}$ for $\varepsilon_1 < \varepsilon < \infty$ and $n_{\text{ph}} = 0$ for $\varepsilon \leq \varepsilon_1$. Solid curves: $\varepsilon_1 = 1$ eV; dashed curves: $\varepsilon_1 = 10^{-3}$ eV. Three different optical depth are shown: $\tau_{\text{max}} = 0.5$ (blue), 3 (green), 6 (red). *Bottom panel:* Variations of the local photon index of the gamma-ray spectrum.

ing of the spectrum due to intergalactic absorption. This is demonstrated in Figs.3 and 4. For the EBL flux we use a “reference” shape close to the one calculated by Primack et al. (2005), but with two different absolute flux normalizations at the wavelength $\lambda = 2.2\mu\text{m}$: $u_{\text{EBL}}(2.2\mu\text{m}) = 16$ nW/m²sr (Fig.3) and 32 nW/m²sr (Fig.4). The first flux is a factor of two larger than the low-limit of EBL corresponding to the integrated light contributed by resolved galaxies (Madau and Pozzetti 2000), while the second flux can be treated as an upper limit at $2.2\mu\text{m}$ (it is slightly higher than the fluxes claimed from the COBE/DIRBE and 2MASS measurements (Wright et al. 2001; Cambresy et al. 2001). Note that for the primary (unabsorbed) differential gamma-ray spectrum with a photon index $\Gamma_0 = 2$, the attenuation factor $\kappa = \exp(-\tau)$ describes the SED of the absorbed radiation ($E^2 dN/dE \propto \kappa(E)$). All curves are obtained for a source located at $z = 0.186$. This is the redshift of the BL Lac object 1ES 101-232, the gamma-ray observations of which by the HESS collaboration have been initially used to constrain the EBL flux at optical and NIR wavelengths (Aharonian et al. 2006a).

The solid curves in Figs.3 and 4 (marked as “d”) correspond to the pure intergalactic effect (i.e. without the internal absorption). They show strong steepening of the spectrum below 1 TeV and above 10 TeV with a noticeable recovery of the initial shape around a few TeV, which is explained by the specific shape of the EBL energy flux (close to $u_{\text{EBL}} \propto \lambda^{-1}$) between 2 and $10\mu\text{m}$ (Aharonian 2001). It is seen that for the absolute flux of EBL with a normalization at $2.2\mu\text{m}$,

$u_{\text{EBL}}(2.2\mu\text{m}) = 16$ nW/m²sr, the photon index between 100 GeV and several TeV is changes by $\Delta\Gamma \sim 2$, thus, the intrinsic (source) spectrum should be very hard with a slope $\Gamma = \Gamma_{\text{obs}} - \Delta\Gamma \sim 1$, where $\Gamma_{\text{obs}} = 2.88 \pm 0.17$ is the observed photons index of 1ES 101-232 (Aharonian et al. 2006a). Postulating that the photon index allowed by conventional models of gamma-ray production in blazars should not exceed $\Gamma_0 = 1.5$, an upper limit on the EBL flux, at the level of $u_{\text{EBL}}(2.2\mu\text{m}) \approx 10$ nW/m²sr has been derived by the HESS collaboration (Aharonian et al. 2006a). It is seen from Fig.3 that this upper limit can be readily increased by a factor of 1.5, allowing a substantial internal absorption of gamma-rays. Indeed, the “joint operation” of internal and intergalactic absorptions results in the changes of the slope of the initial gamma-ray spectrum in the relevant energy band by $\Delta\Gamma \sim 0$ to 1.5 for $\tau_{\text{max}} = 3$, and $\Delta\Gamma$ from -0.5 to +0.5 for $\tau_{\text{max}} = 6$. In the latter case, the overall change of the shape of the initial spectrum from 100 GeV to 5 TeV is quite small, so hard TeV gamma-ray spectra can in principle be detected also from distant blazars. This assumption can solve, to a certain extent, the problem related to the spectra of accelerated (parent) particles, and thus (unfortunately!) relax the constraints on the EBL that can be derived from gamma-ray observations. Formally, a detection of not-very-steep TeV gamma-ray spectra with $\Gamma_{\text{obs}} \leq 4$ from distant ($z \geq 0.15$) blazars cannot be excluded even for an EBL flux close to the claimed high EBL fluxes derived from the COBE/DIRBE and 2MASS measurements (Cambresy et al. 2001), $u_{\text{EBL}}(2.2\mu\text{m}) \approx 28$ nW/m²sr. This is demonstrated in Fig.4. At energies above 300 GeV the absorption of gamma-rays in EBL only increases the photon index by $\Delta\Gamma \geq 4$, while an additional internal absorption with $\tau_{\text{max}} = 10$ results in $\Delta\Gamma \leq 2$. Approximately the same result is expected for low EBL (e.g. at the level of $u_{\text{EBL}}(2.2\mu\text{m}) = 10$ nW/m²sr), but for sources located at $z \gg 0.1$. In this regard, the recent claim of detection of VHE gamma-rays from 3C 279 ($z = 0.538$) by the MAGIC collaboration (Teshima et al. 2007) can be an indication of significant gamma-ray absorption inside the source. Otherwise, even for the minimum possible EBL flux, the pure intergalactic absorption would result in an extremely steep VHE gamma-ray spectrum with a photon index ≥ 5 . It is interesting to note that the UV photons of the broad-line emission region of a size $R \sim 10^{17}$ cm and luminosity $L \sim 2 \times 10^{44}$ erg/s (Pian et al. 2005) can serve as a perfect target for internal absorption of high energy gamma-rays in 3C 279.

The internal absorption of gamma-rays significantly increases the energy requirements to the source. For example in the case of $\tau_{\text{max}} = 5$, the internal absorption leads to the reduction of the observed flux at 1 TeV by an additional factor of 10. This, combined with the intergalactic absorption, implies 3 orders of magnitude attenuation of the primary radiation (see Fig.3). For the quiescent state of 1ES 101-232, the corresponding apparent gamma-ray luminosity around 1 TeV is estimated $L_{\text{TeV}} \simeq 10^{44} \kappa^{-1}$ erg/s. For the attenuation factor $\kappa(1\text{ TeV}) \sim 10^{-3}$, it becomes huge, 10^{47} erg/s, and perhaps one or two orders of magnitude even larger in the flaring states (in analogy with

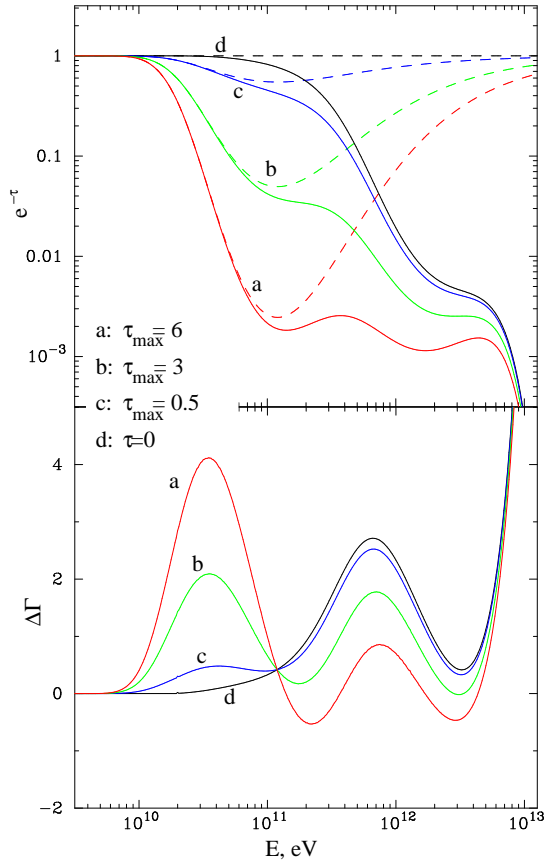


Figure 3. Internal and intergalactic absorption of gamma-rays. *Upper panel:* Attenuation factors. The internal absorption is calculated for a Planckian distribution of target radiation with temperature $T = 5 \times 10^4$ K. Three dashed curves correspond to the internal optical depths $\tau_{\max} = 6$ (a) 3 (b), 0.5 (c), 0 (d). The corresponding solid curves include both the internal and intergalactic absorption. The intergalactic absorption is calculated for a source at $z = 0.186$ (the redshift of the BL Lac object 1ES 101-232), assuming a reference shape of the EBL spectrum close to the one calculated by Primack et al. (2005), and normalized to the EBL flux at $2.2 \mu\text{m}$: $u_{\text{EBL}}(2.2 \mu\text{m}) = 16 \text{ nW/m}^2\text{sr}$. *Bottom panel:* Variation of the local photon index.

Mkn 421, Mkn 501 and PKS 2155-304)¹. Nevertheless, since there is little doubt that gamma-rays are produced in relativistically moving jets with a Doppler factor $\delta \geq 30$ or even ≥ 100 , as it follows from the recently reported variability of Mkn 501 (Albert et al. 2007) and PKS 2155-304 (Aharonian et al. 2007b) on minute scales (see e.g. Fabian et al. (2007)), the intrinsic luminosity $L_{\text{int}} = L_{\text{app}}\delta^{-4}$, could be quite modest, namely, at the level of $10^{39} - 10^{41} \text{ erg/s}$ which, in fact, is not far from the TeV gamma-ray luminosity of the nearby non-blazar type AGN M87 (Aharonian et al. 2006b).

The attenuation of TeV gamma-rays dramatically increases the intrinsic TeV to GeV gamma-ray flux ratio. This does not, however, contradict the GeV flux upper limits

¹ The detected gamma-ray flux around 200 GeV is an order of magnitude larger than at 1 TeV, however, because of dramatic reduction of the absorption effect, the contribution of low energies to the (absorption-corrected) apparent luminosity, is relatively small.

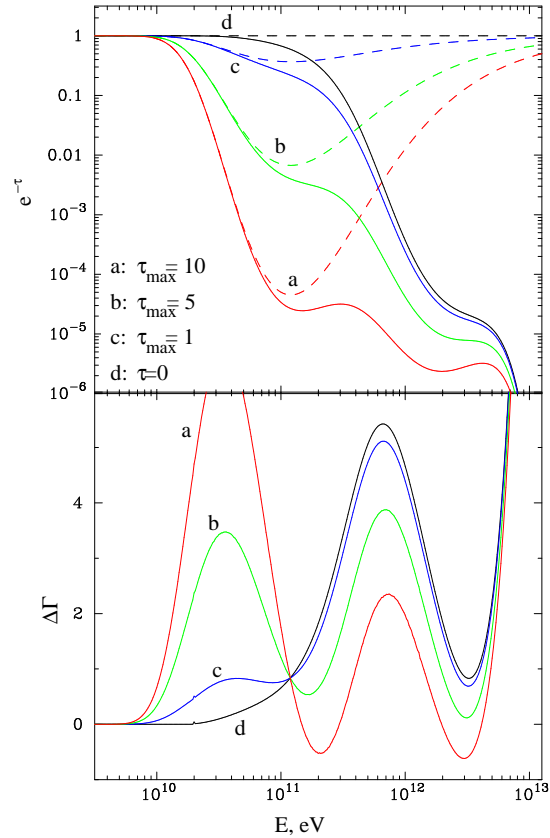


Figure 4. The same as in Fig. 3, but the curves are calculated for the internal optical depths 10 (a), 5 (b), 1 (c) and 0 (d). For EBL flux is assumed twice larger than in Fig. 3: $u_{\text{EBL}}(2.2 \mu\text{m}) = 32 \text{ nW/m}^2\text{sr}$.

available from the EGRET observations (typically, at the level of $10^{-10} \text{ erg/cm}^2\text{s}$ or higher), especially if one takes into account that the energy spectra of gamma-rays produced in some principal radiation processes (e.g. through inverse Compton scattering or proton synchrotron radiation) at sub-TeV energies are expected harder than E^{-2} . On the other hand, we certainly expect GeV gamma-rays from TeV blazars, and in this respect, the upcoming GLAST measurements with significantly improved (compared to EGRET) sensitivity, especially at multi-GeV energies, should provide the first effective probes of TeV blazars in the MeV/GeV domain in general, and for the “internal gamma-ray absorption” scenario, in particular.

Finally, in the case of hadronic origin of TeV gamma-rays produced at pp and/or $p\gamma$ interactions, the flux of accompanying TeV neutrinos, which freely penetrate through the internal and extragalactic radiation fields, can be as high as $10^{-10} \text{ neutrinos/cm}^2\text{s}$, i.e. above the detection threshold of the next generation km^3 scale neutrino detectors. The detection of both gamma-rays and neutrinos from TeV blazars, and the comparison of fluxes of these two components of radiation would provide principal information about the high energy processes in blazars, as well as about the attenuation of gamma-rays due to the (combined) internal and intergalactic absorption. An additional information about the internal photon-photon absorption alone (separated from the

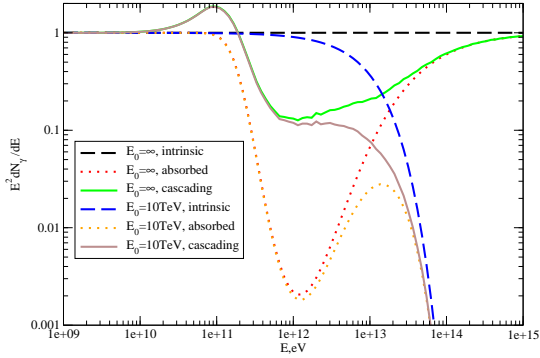


Figure 5. Gamma-ray spectra caused by the internal photon-photon absorption (dotted curves) or formed during a development of pair cascades (solid curves) in a radiation field with temperature $T = 10^4$ and optical depth $\tau_{\max} = 6$. It is assumed that the energy density of radiation significantly exceeds the energy density of the magnetic field, $u_r \gg u_B$. The spectra of primary gamma-radiation (dashed lines) are assumed as “power-law with exponential cutoff”: $dN/dE \propto E^{-2} \exp(-E/E_0)$ with $E_0 = 10$ TeV and $E_0 = \infty$.

extragalactic absorption) is contained in the radiation of secondary (pair-produced) electrons.

3 RADIATION OF SECONDARY ELECTRONS

The propagation of high energy gamma-rays through a low-energy photon field cannot be reduced to the simple effect of absorption. When the gamma-ray photon is absorbed, its energy is transferred to the electron-positron pair. The secondary electrons interacting with the ambient magnetic and radiation fields produce high energy photons, either via synchrotron radiation or inverse Compton scattering. The synchrotron photons are produced with much smaller energies, thus they do not interact with the background low-energy photons. In a target field with narrow spectral distribution, inverse Compton scattering of the photo-produced electrons proceeds in the Klein-Nishina limit; the upscattered photon receives the major fraction of the electron energy, thus is able to interact again with background photons. The second generation pairs again produce gamma-rays, thus an electromagnetic cascade develops.

While the energy of gamma-rays interacting with EBL dissipates in the intergalactic medium, and in this way contributes to the diffuse extragalactic background radiation, the secondary radiation caused by internal absorption may accompany the primary (unabsorbed) fraction of gamma-rays. In this regard, the development of an electromagnetic cascade is not a desirable process, because it masks the distinct absorption features, and thus prevents the formation of very hard gamma-ray spectra. This is demonstrated in Fig. 5. The cascade spectra are calculated assuming that the region of production of primary gamma-rays is located in the center of a spherical source filled with grey-body radiation with temperature $T = 10^4$ K and optical depth $\tau_{\max} = 6$. The spectrum of primary gamma-rays is given in the form: $dN/dE \propto E^{-2} e^{-E/E_0}$ for two values of the cutoff energy: $E_0 = 10$ TeV and $E_0 = \infty$. In Fig. 5 both the absorbed and cascade gamma-ray spectra are shown. It is seen that

the development of pair cascades fully washes out the absorption features, and instead forms a standard spectrum with a maximum (“bump”) around the interaction threshold, $\sim (m_e c^2)^2 / kT \sim 100$ GeV, followed by a steep spectrum above the “bump”. The cascade spectrum around 1 TeV saturates at the level of 10 percent of the primary gamma-ray flux. The spectrum above 1 TeV has a flat shape until the efficiency of the cascade drops (because of the progressively decreasing optical depth) with a gradual transition to the “absorption” regime.

There are two ways of significant reduction of the contribution from the cascade component to the observed gamma-radiation.

(i) *Absorption of gamma-rays outside the production region.* In this case the “foreground” cascade radiation cannot screen the unabsorbed fraction of gamma-rays. Indeed, although the energy in the cascade radiation exceeds, by a factor of 100, the energy of the unabsorbed fraction of primary radiation (see Fig. 5), for the observer the primary radiation emitted by a relativistically moving source (“blob”) will be much brighter ($\propto \delta_j^4$) and shifted to higher energies ($\propto \delta_j$) compared to the isotropic cascade emission of the surrounding environment. On the other hand, the part of the cascade developed inside the blob is, of course, also Doppler boosted, therefore the condition of suppression of the cascade component can be satisfied when the optical depth within the blob $\tau' \ll 1$, i.e. the gamma-ray production region is much smaller than the source of the optical/UV radiation, $l \ll R$. Since the gamma-ray production regions in blazars are believed to be very compact, $l \sim 10^{14} - 10^{16}$ cm, we may conclude that the source of the optical radiation should be larger than $R \sim 10^{15} - 10^{17}$ cm. There are many potential sources of optical radiation in blazars (see e.g. Urry and Padovani 1995). In this paper we do not intend to specify the origin of the low-energy radiation fields, but simply notice that an even modest optical source located in the core of a blazar can provide an effective target for gamma-ray absorption. The luminosity of this source is estimated as $L_O = 12\pi n_{ph} kTR^2 c$, where n_{ph} is the average number density of radiation. It can be estimated from the condition $\sigma_{\gamma\gamma} R n_{ph} = \tau_{\max}$. For a characteristic optical depth $\tau_{\max} \sim 5$ and temperature $T = 5 \times 10^4$ K, we obtain, $L_O \simeq 2 \times 10^{43} (R/10^{17} \text{ cm}) \text{ erg/s}$.

(ii) *Secondary electrons cooled through synchrotron radiation.* This condition can be satisfied if the energy density of the magnetic field exceeds the energy density of radiation, $B^2/8\pi \geq 3kTn_{ph}$ or $B \geq 0.4(R/10^{17} \text{ cm})^{-1/2}$ G. In Fig. 6 the broad-band SED of the radiation initiated by absorption of primary gamma-rays with a power-law spectrum $dN/dE \propto E^{-2}$ is shown, assuming that the absorption of gamma-rays takes place inside the gamma-ray production region. Calculations are performed for three different optical depths $\tau_{\max} = 0.5, 3$, and 6 , a fixed temperature of radiation $T = 5 \cdot 10^4$ K, and two extreme values of the magnetic field, $B = 100$ G and $B = 0.1$ G. In calculations of the electron spectra we assume that the energy losses of electrons are dominated by synchrotron cooling. Note that the spectrum of synchrotron radiation of secondary electrons has a characteristic bell-type form, i.e. quite similar to the synchrotron spectra formed in the synchrotron-self Compton (SSC) models. However, in the SSC models designed for TeV blazars

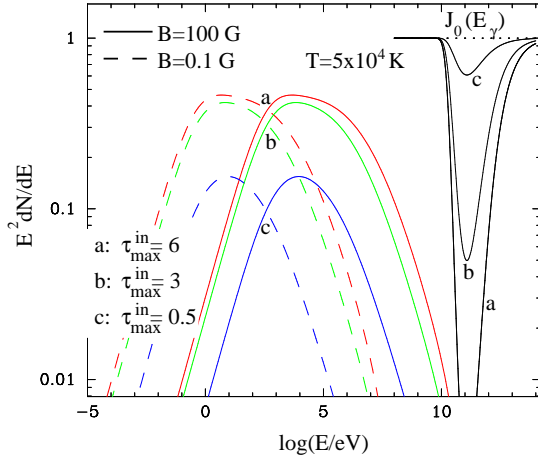


Figure 6. Synchrotron radiation of secondary electrons. The primary gamma-ray spectrum is assumed $dN/dE \propto E^{-2}$ (dotted line). The target photon field is Planckian with $T = 5 \cdot 10^4$ K. The absorbed gamma-ray spectra and the corresponding spectra of secondary electrons are calculated for three optical depths $\tau_{\max}^{\text{in}} = 6$ (a), 3 (b), and 0.5 (c). The synchrotron radiation is calculated assuming that the absorption of gamma-rays takes place inside the source (gamma-ray production region) for two values of the magnetic field: $B = 100$ G (solid curves) and $B = 0.1$ G (dashed curves).

the synchrotron peak is a result of the maximum energy of accelerated electrons, while the hard low-frequency part of the spectrum is determined by radiation of uncooled low-energy electrons. In the "internal gamma-ray absorption" scenario we see similar features, but for different reasons. The electrons in a narrow-band radiation field are produced with a spectrum similar to the spectrum of parent gamma-rays ($\propto E^{-\Gamma_0}$), but with cutoffs both at low- and high energies. These cutoffs are explained by the threshold of the photon-photon pair production and by the reduction of its cross-section at highest energies, respectively. Due to the synchrotron cooling, at low energies the electron spectrum obtains a standard $\propto E^{-2}$ form, which gradually transforms to a $\propto E^{-(\Gamma_0+1)}$ type spectrum at intermediate energies and a cutoff at highest energies. The corresponding spectral features are reflected in the synchrotron spectrum - a power-law with a photon index 1.5 at low energies, with a smooth transition to a power-law with a photon index $\Gamma_0/2+1$ at intermediate energies, and a smooth gradual cutoff at highest energies. A significant difference between the SSC and the "internal gamma-ray absorption" models appears also in the ratio of fluxes corresponding to the low (IR to X-ray) and high (gamma) energy peaks. While in the SSC scenario this ratio is determined by the ratio of energy densities of the magnetic and target photon fields, in the "internal gamma-ray absorption" scenario this ratio is basically determined by the efficiency of gamma-ray absorption inside the source. The magnetic field determines only the position of the synchrotron peak, but not the flux level. The latter is determined by the factor proportional to $(1 - \exp[-\tau_{\max}])$. For $\tau_{\max} \gg 1$, the dependence on the optical depth almost disappears. All these features can be seen in Fig. 6.

The position of the synchrotron peak depends, in a quite interesting way, also on the Lorentz and Doppler factors of the source. While in the standard models of blazars the

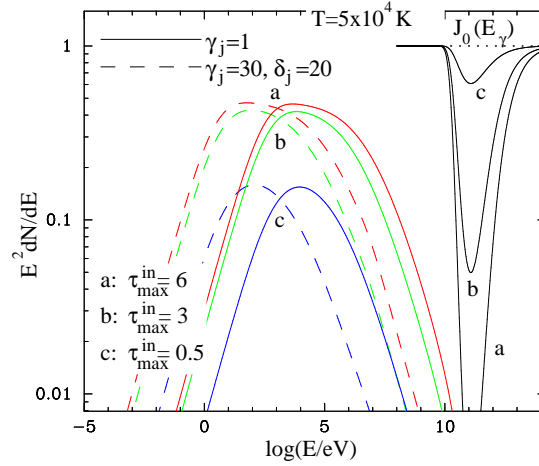


Figure 7. Impact of the bulk motion on synchrotron radiation of secondary electrons. The magnetized blob moves with a relativistic velocity. The synchrotron maximum moves by a factor of δ_j/γ_j^2 and the distributions become somewhat wider. The primary gamma-ray spectrum was assumed power-law: $\propto E_\gamma^{-2}$ (is shown by the dotted line). The target photon field is Planckian with $T = 5 \cdot 10^4$ K. The absorbed spectra are shown by black solid curves for $\tau_{\max} = 6$ (a), $\tau_{\max} = 3$ (b) and $\tau_{\max} = 0.5$ (c). We calculate synchrotron radiation from a magnetized region with the average optical depth (over different directions) $\tau_{\max}^{\text{in}} = 6$ (a, red lines), 3 (b, green lines) and 0.5 (c, blue lines). The magnetic field is assumed $B = 100$ G. Calculations are performed for two different bulk Lorentz factors: $\gamma_j = 1$ (no motion) and $\gamma_j = 30$ (for $\delta_j = 20$).

Doppler effect shifts the overall SED towards higher energies by a factor of δ_j , in the "gamma-ray absorption" scenario the synchrotron peak is shifted towards lower energies (see Fig. 7). The reason is quite simple. In the frame of the relativistically moving source illuminated by an external radiation with a characteristic energy ε_0 , the electrons are produced with energies $E_{\min} \geq (m_e c^2)^2 / (\varepsilon_0 \gamma_j)$, thus the position of the synchrotron peak in the frame of the observer is proportional to $\delta_j E_{\min}^2 \propto \delta_j / \gamma_j^2$. Thus in a source moving towards the observer at a small angle, the position of the synchrotron peak in the frame of the observer is inversely proportional to the Doppler factor δ_j , just opposite to the spectrum of gamma-rays which is shifted towards higher energies by the same Doppler factor.

The position of the synchrotron peak depends strongly also on the average energy (or temperature) of the target radiation field. Indeed, with an increase of the temperature of background radiation T , the threshold of photon-photon interactions, and consequently the minimum energy of produced secondary electrons decreases as $E_{\min} \propto 1/T$, and hence the synchrotron peak moves towards lower energies as $h\nu_m \propto 1/E_{\min}^2 \propto 1/T^2$. Generally, the position of the synchrotron peak of pair produced electrons depends on the temperature of the target radiation field, the magnetic field, and the Doppler and Lorentz factors of the jet, as

$$h\nu_m \propto BT^{-2}(\delta_j/\gamma_j^2). \quad (3)$$

It is easy to derive a simple analytical expression which described the high energy part of the synchrotron spectrum, $h\nu \gg h\nu_m$, produced by electrons for which the source becomes optically thin, $\tau(E) \leq 1$. In this case the produc-

tion spectrum of electrons $Q(E) \propto 1/EdN_\gamma/dE$ (here we ignore the weak logarithmic term in the photon-photon interaction cross-section). Then, for the power-law gamma-ray spectrum, $dN_\gamma/dE \propto E^{-\Gamma_0}$, the cooled electron spectrum is also power-law, $dN_e/dE_e \propto E^{-\Gamma_0-2}$, and correspondingly the SED of synchrotron radiation, $\nu F_\nu \propto \nu^{-(\Gamma_0+1)/2}$. For example, for $\Gamma_0 = 2$, the SED of synchrotron radiation is rather steep, $\nu F_\nu \propto \nu^{-1.5}$. In fact, because of the cutoff in the gamma-ray spectrum, the high energy tail of synchrotron radiation is expected even steeper. This is demonstrated in Fig. 8 where the broad-band SEDs of radiation initiated by gamma-rays in a source at $z = 0.186$ are shown. It is assumed that gamma-rays in the frame of the jet moving with a Lorentz factor $\gamma_j = 10$ have a power-law distribution with an exponential cutoff at 1 TeV, $dN_\gamma/dE \propto E^{-3/2} \exp(-E/1\text{TeV})$. It is assumed also that $\delta_j = \gamma_j$ (i.e. the viewing angle is $\theta \approx 6^\circ$). The calculations are performed for two temperatures of the radiation field through which the jet propagates - $T = 5 \times 10^4$ K and $T = 5 \times 10^5$ K, assuming that in both cases the optical depth inside the moving gamma-ray production region (the blob) with a homogeneous magnetic field is $\tau_{\text{max}} = 3$. Finally for the intergalactic absorption a "template" EBL spectrum is assumed with a normalization at $2.2 \mu\text{m}$ at the level of $16 \text{ nW/m}^2\text{ster}$. The impact of the temperature on both the spectrum of arriving gamma-rays and the synchrotron radiation of secondary electrons is clearly seen. Note that while below 100 GeV the deformation of the primary gamma-ray spectrum is caused mainly by internal absorption, the sharp cutoff at energies above 10 TeV is due to the severe intergalactic absorption. In the intermediate energy range between 100 GeV and 10 TeV the internal and intergalactic photon-photon interactions "operate" together resulting in quite specific broad-band SEDs. The discussion of implications of these results for specific astrophysical objects is beyond the scope of this paper. We note only that our preliminary studies show that the suggested model in general can satisfactorily explain the observed broad-band SEDs of TeV blazars.

4 DISCUSSION

The energy spectra of VHE gamma-rays from blazars, after correction for intergalactic absorption, generally appear very hard, even for the minimum flux level of EBL determined by the integrated light of resolved galaxies at optical (Hubble) and infrared (Spitzer) wavelengths. A slight deviation from the robust lower limits of EBL leads to unusually hard intrinsic gamma-ray spectra which cannot be easily explained within the standard particle acceleration and radiation models. In this paper we suggest a scenario which can lead to the formation of intrinsic gamma-ray spectra of arbitrary hardness without introducing modifications in the particle acceleration models. The main idea is that the gamma-rays before they leave the source suffer significant internal energy-dependent absorption due to interactions with the ambient low-frequency photons. The existence of dense radiation fields of different origin in blazars (see e.g. Urry and Padovani (1995)) combined with the large photon-photon pair production cross-section, makes this scenario quite natural and effective, in particular in the compact

cores of blazars. For the formation of hard VHE gamma-ray spectra, the target radiation field must have a rather narrow spectral distribution or a sharp low-energy cutoff, with a typical energy of photons of about 1 to 10 eV. Formally, for very large optical depths, this process can provide an arbitrary hardness of gamma-ray spectra, though at the expense of a significant increase of the required nonthermal energy budget. However, as long as the current blazar models require relativistically-moving gamma-ray production regions with large Doppler factors, $\delta_j \geq 30$, and perhaps even more (Aharonian et al. 2007b; Fabian et al. 2007), the available energy budget seems to be not a critical issue.

The unavoidable feature of the proposed model is the radiation of secondary electrons via synchrotron or inverse Compton scattering. If the optical depth inside the gamma-ray production region is small, $\tau \ll 1$, e.g. the gamma-ray source is much smaller than the external source of optical photons, the secondary electrons are produced and radiate mainly outside the gamma-ray production region. Even in the case of heavy absorption of gamma-rays, the secondary radiation of secondary electrons can hardly be detected. Indeed, since the intrinsic gamma-ray luminosity is relatively modest, and the absorbed energy is re-radiated as an isotropic source², the lost of the beaming factor dramatically reduces the signal compared to the primary (Doppler boosted) radiation.

The picture is dramatically changed when the gamma-ray source moves through a very dense photon field, such that the optical depth inside the source becomes larger than 1. In this case the main fraction of the absorbed energy is released in the form of secondary electrons inside the gamma-ray production region, and thus the radiation of the secondary electrons profits, as the primary gamma-radiation does, from the Doppler boosting. The secondary electrons are cooled through synchrotron and/or inverse Compton channels. The latter in fact proceeds via development of pair cascades as long as the typical energies of electrons or gamma-rays and the energy of target photons $\varepsilon E_{e,\gamma} \gg m_e^2 c^4$. The cascade, however, diminishes the energy-dependent absorption features, thus the model becomes effective when the electrons are cooled predominantly via synchrotron radiation, i.e. $B^2/8\pi \geq u_r$. The energy density of the radiation $u_r = \bar{\varepsilon} n_{\text{ph}}$ with an average energy of target photons of about $\bar{\varepsilon} \sim 1$ eV is estimated from the condition $\tau_{\text{max}} \geq 1$, thus for the effective suppression of the cascade

$$B \geq (40\pi\bar{\varepsilon}/\sigma_T l)^{1/2} \approx 0.5(l/10^{15}\text{cm})^{-1/2}\tau_{\text{max}}^{1/2} \text{ G} \quad (4)$$

For an optical depth $\tau_{\text{max}} \sim 1$ and the size of the gamma-ray source $l \sim 10^{16}$ cm, the magnetic field exceeding 0.1 G should be sufficient to prevent the cascade. For smaller gamma-ray production regions, e.g. $l \sim 10^{14}$ cm, the magnetic field should be larger than 1 G. For such magnetic fields the synchrotron radiation of secondary electrons appears in the optical to hard X-ray energy bands. Depending on the optical depth, the synchrotron peak can be higher than the gamma-ray peak. Interestingly, unlike the classical "synchrotron/Inverse-Compton" models, where the ra-

² Unless the electrons are produced in an environment with a very low magnetic field, and thus are cooled via inverse Compton scattering before any noticeable deflection.

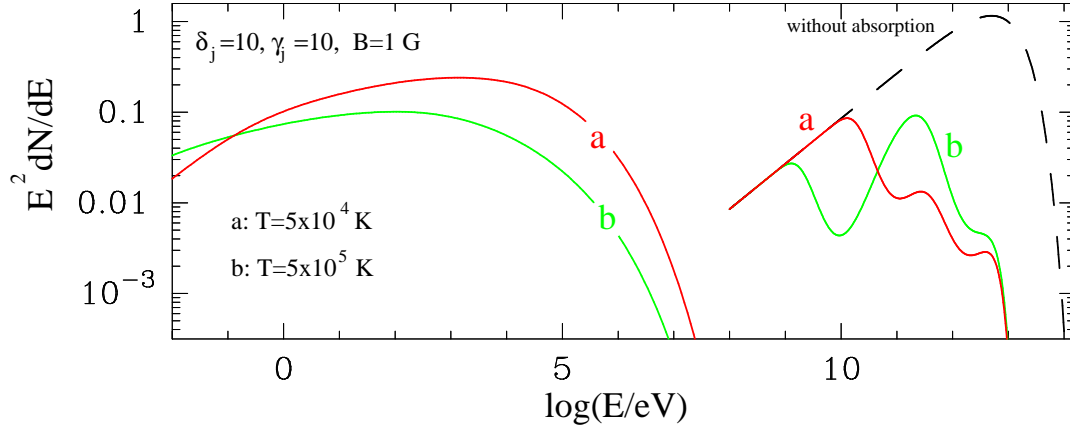


Figure 8. Impact of the radiation temperature on the spectral energy distribution of emission initiated by primary gamma-rays in a jet moving through a homogeneous radiation field. The source is located at $z = 0.186$. The dashed curve is the assumed primary spectrum of gamma-rays. The solid curves represent the synchrotron radiation of the secondary electrons as well as the gamma-ray spectra after the internal and extragalactic absorption. Calculations are performed for two radiation temperatures, $T = 5 \times 10^4$ K (a) and $T = 5 \times 10^5$ K (b). For both cases $\delta_j = \gamma_j = 10$, $B = 1$ G, $\tau_{\max} = 3$. An EBL is assumed with a normalization of the flux $u_{\text{EBL}}(2.2\mu\text{m}) = 16$ nW/m²str.

tio of the synchrotron to IC peak is determined by the ratio u_B/u_r , in the "internal gamma-ray absorption" scenario the synchrotron peak does not strongly depend on the magnetic field. Whether this scenario can be applied to the broad-band SEDs of gamma-ray blazars, is an interesting issue which requires special dedicated studies.

Finally, we want to discuss briefly the radiation mechanisms of primary gamma-radiation. Generally, the model does not give a preference to the leptonic or hadronic origin of radiation, unless the magnetic field exceeds the estimate given by Eq.(4). In this case the synchrotron-to-IC flux ratio produced by directly accelerated electrons would be too high, especially after the internal absorption of gamma-rays, contrary to the detected SEDs of most of the TeV blazars.

Large magnetic fields in the gamma-ray production region, typically $B \geq 1$ G, would favor gamma-ray production by relativistic protons, with all advantages and disadvantages common for hadronic models. The basic problem of hadronic models is linked to the low interaction rates which do not allow the most natural explanation of the observed fast gamma-ray variability of blazars in terms of radiative cooling. For example, in the case of interactions of protons with the ambient plasma with number density n , the characteristic time of pp interactions with production of π^0 -mesons is $t_{pp} \approx 10^{15} n^{-1}$ s. Thus, in order to explain the variability of gamma-rays as short as several minutes like the TeV flares observed from PKS 21555-301 and Mkn 501, the density of plasma should be as large as $5 \times 10^{12} \delta_j^{-1} \text{ cm}^{-3}$ which implies a very heavy source and correspondingly huge kinetic energy $E_{\text{kin}} = (4/3)\pi l^3 n m_p c^2 \gamma_j \approx 10^{55}$ erg (here we assume that $\delta \approx \gamma_j$). One may invoke alternative explanations of the variability of blazars, e.g. due to the adiabatic losses or escape of particles from the source, but this assumption leads to dramatic reduction of radiation efficiency, and to an increase the energy requirements to the accelerated protons.

A similar problem face the photomeson processes at interactions of protons with the ambient radiation fields. Actually in the "internal gamma-ray absorption" scenario this mechanisms seems a quite natural choice because the same background photons which absorb gamma-rays can

play a role of the target for photomeson interactions. However, because of the small cross-section, the efficiency of this process again appears quite low. The interaction time of protons with energy, $E \geq 200$ MeV ($\bar{\epsilon} \gamma_j$) $\simeq 2 \times 10^{16} (\bar{\epsilon}/1 \text{ eV})^{-1} (\gamma_j/10)^{-1} \text{ eV}$ (in the frame of the moving source with a Lorentz factor γ_j) is estimated $t_{p\gamma} \approx 1/(f \sigma_{p\gamma} n_{\text{ph}} c) \sim (\sigma_{\gamma\gamma}/\sigma_{p\gamma}) f^{-1} R/c \tau_{\max}^{-1}$ ($< \sigma_{p\gamma} > \approx 10^{-28} \text{ cm}^2$ is the average cross-section and $f \sim 0.2$ is the multiplicity of the process). Thus, we can see that during the passage of the source of optical photons of size R , the protons transfer only $\sigma_{p\gamma}/\sigma_{\gamma\gamma} \sim 10^{-3}$ fraction of their energy to gamma-rays. If such a low efficiency can be compensated by very large Doppler boosting (e.g. assuming $\delta_j \sim 100$), this channel can provide very large fluxes of neutrinos, which unlike gamma-rays do not suffer internal and extragalactic absorption. In the case of attenuation of VHE gamma-ray fluxes by 2 to 3 orders of magnitude, the expected fluxes of neutrinos from TeV blazars can be as large as the detection threshold of the km³ volume high energy neutrino telescopes, $F_{\nu_\mu} (\geq 1 \text{ TeV}) \approx 10^{-11} \text{ neutrinos/cm}^2 \text{ s}$.

It is interesting to note that, because of the threshold of photomeson production, the interactions of protons of arbitrary distribution with a narrow band radiation with a characteristic energy $\bar{\epsilon}$, result in a differential gamma-ray spectrum which below the energy $\approx 10^{16} (\bar{\epsilon}/1 \text{ TeV})^{-1} \text{ eV}$ is extremely hard, $dN/dE = \text{const}$, thus this process itself can provide very hard gamma-ray spectra independent of the spectrum of parent protons.

Despite certain attractive features, this mechanism faces the same problem as pp interactions - a low radiation efficiency. Therefore it can work only under conditions of extremely large Doppler boosting of radiation. The efficiency of VHE gamma-ray production can be much higher in the case of synchrotron radiation of protons, provided that the acceleration of protons proceeds at a rate close to the fundamental limit, and the magnetic field in the proton accelerator well exceeds 10 G. In particular, in the magnetic field of order 100 G, protons can be accelerated to energies 10^{20} TeV and thus can produce VHE synchrotron gamma-rays on timescales of 10^4 s. Although due to the

self-regulated synchrotron cutoff (Aharonian 2000) the spectrum of gamma-rays is limited by sub-TeV energies, an observer detects Doppler boosted gamma-radiation extending to multi-TeV energies. The characteristic feature of this mechanism is the very large electromagnetic energy contained in the blob, $1/6l^3 B^2 \approx 2 \times 10^{48}$ erg, hard X-ray emission of the secondary (pair-produced) electrons, and negligible fluxes of neutrinos.

REFERENCES

- Aharonian, F.A. et al (HEGRA collaboration), 1999, A&A, 349, 11
- Aharonian, F.A., 2000, New Astronomy, 5, 377
- Aharonian, F.A., 2001, Invited, Rapporteur and Highlight Papers., Proc. 27th ICRC, Edited by R. Schlickeiser, Hamburg
- Aharonian, F.A., Timokhin, A.N., and Plyasheshnikov, A.V. 2002, A&A, 384, 834
- Aharonian, F.A., 2004, High Energy Cosmic Radiation: a window on the extreme Universe, World Scientific.
- Aharonian, F.A. et al. (HESS collaboration), 2006, Nature, 440, 1018
- Aharonian, F.A. et al. (HESS collaboration), 2006, Science, 314, 1424
- Aharonian, F.A. et al. (HESS collaboration), 2007, A&A, 475, L9
- Aharonian, F.A. et al. (HESS collaboration), 2007, ApJ, 664, L71
- Albert, J. et al., 2007, ApJ, 669, 862
- Cambresy, L., Reach, W.T., Beichman, C.A., and Jarret, T.H., 2001, ApJ, 555, 563
- Dole, H. et al. 2006, A&A, 451, 417
- Fabian, A., Begelman, M., and Rees, M.J.. 2007, MNRAS, in press.
- Fazio, G. G. et al., 2004, ApJS, 154, 39
- Finkbeiner, D.P., Devis, M., and Schlegel, D.J., 2000, ApJ, 544, 81
- Gould, R.J. and Schröder, G.P., 1967, Phys. Rev., 155, 1408.
- Hauser, M.G. et al., 1998, ApJ, 508, 25
- Hauser, M.G., and Dwek, E., 2001, ARA&A, 39, 249
- Hinton, J., 2007, arXiv:0712.3352
- Jelley, J.V., 1966, Phys. Rev. Letters, 16, 479
- Kashlinsky, A., 2005, Phys. Rep., 409, 361.
- Katarzynski, K., Ghisellini, G., Tavecchio, F., Gracia, J., Maraschi, L. 2006, MNRAS, 368, L52
- Kifune, T., 1999, ApJ, 518, L21
- Lagage, G. et al., 1999, A&A, 344, 322
- Nikishov, A.I., 1962, *Sov. Phys. JETP*, 14, 393.
- Madau, P., and Pozzetti, L., 2000, MNRAS, 312, 9
- Mappelli, M., Salvaterra, R., Ferrara, A., 2006, New Astronomy, 11, 420
- Mazin, D., and Raue, M., 2007, A&A, 471, 439
- Pian, E., Falomo, R., Treves, A., 2005, MNRAS, 361, 919
- Protheroe, R.J., and Meyer, H., 2000, Physics Letters B, 493, 1
- Primack, J., Bullock, J.S., and Somerville, R.S., 2005, AIP conf. Proceedings, 745, 23
- Schlegel, D.J., Finkbeiner, D.P., and Davis, M., 1998, ApJ, 500, 525
- Teshima, M. et al., 2007, arXiv:0709.1475v1
- Urry, C.M. and Padovani, P., 1995, PASP, 107, 803
- Wright, E.L., 2001, ApJ, 555, 538.